Dual Redox and Optical Control of Chiroptical Activity in Photochromic Dithienylethenes Decorated with Hexahelicene and Bis-Ethynyl-Ruthenium Units

Chengshuo Shen, Xiaoyan He, Loic Toupet, Lucie Norel, Stéphane Rigaut, Jeanne Crassous

Dual redox and optical control of chiroptical activity in photochromic dithienylethenes decorated with hexahelicene and bis-ethynyl-ruthenium units.

Chengshuo Shen, [†] Xiaoyan He,[†] Loïc Toupet,[†] Lucie Norel,[†] Stéphane Rigaut, [*,†] Jeanne Crassous [*,†]

[†] Institut des Sciences Chimiques de Rennes, UMR 6226, Institut de Physique de Rennes, UMR 6251, Campus de Beaulieu, CNRS-Université de Rennes 1, 35042 Rennes Cedex, France

Supporting Information Placeholder

ABSTRACT: We describe the synthesis of mono- and bis-([6]helicene-≡-Ru(dppe)$_2$-≡)-DTE complexes **1o,c** and **2o,c**. The photochromic and electrochromic properties were studied and attractive isomerization processes were observed, ie. spontaneous reopening of [**1c**]$^{+}$ to [**1o**]$^{+}$ and ring closure of [**2o**]$^{2+}$ to [**2c**]$^{2+}$. Due to strong chiroptical responses, all these chiral complexes correspond to new types of chiroptical switches (triggered by light and/or redox stimuli) and could be described as either "NOR" or "OR" logic gates.

INTRODUCTION

Helicenes are molecules formed of *ortho*-fused aromatic rings that adopt a helical shape as a consequence of the steric hindrance between the terminal rings.[1] Such an inherently chiral topology combined with an extended π-conjugation provides helicenes with huge optical rotation (OR) values,[1g] intense electronic circularly dichroism (ECD) spectra[2] substantial circularly polarized luminescence (CPL), under special circumstance described in the literature.[3] As a result of this strong optical activity, helicenes may find applications as chiral molecular materials,[4] especially as chiroptical switches,[5,6] with potential interest as memory elements or logic operators, chiral sensors, encoding elements, switchable asymmetric catalysts or as unidirectional molecular motors.[4b,c] Helicenes display several attractive features to be used as chiroptical switches, such as high thermal stability, higher solubility than more planar aromatic structures and large variations in electronic properties and chiroptical properties upon modification of π-conjugation. In the last decades several types of helicene-based chiroptical switches have been developed, for which the switching process is (i) mainly triggered by light, redox or acid/base stimuli, and (ii) read-out by using one of the chiroptical responses (OR, ECD, CPL).[6]

Among several kinds of photochromic units that can be applied for light-triggered switches, the most widely used is undoubtedly the dithienylethene unit (DTE).[7] Few examples of DTE-based photo-active helicene molecules behaving as light-triggered chiroptical switches have already been described in the literature,[8] such as for instance DTEs bearing two pinene derivatives, for which a stereoselective ring closing process resulted in a DTE-based thia[7]helicene with very large changes in optical rotatory dispersion (ORD) spectra between the open state and the closed photostationary state.[8c]

On the other hand, carbon-rich electroactive ruthenium(II) complexes bearing one or two arylethynyl ligands have been widely studied,[9] and can lead to efficient redox-triggered switches[10] thanks to a reversible redox activity and strong changes in their optical response due to the non-innocent character of the arylethynyl chromophores. Such a concept has been applied by us in the chemistry of organometallic helicenes, notably by grafting on a carbo[6]helicene platform either vinyl-ruthenium or ethynyl-iron redox-active species, and efficient redox-triggered chiroptical switches were obtained.[6a,d,e]

The combination of a photochromic DTE units with redox-active $Ru^{+/0}$ centers through a C≡C bond can generate a multifunctional potential /light-triggered dual switching, either by stimulating oxidation states using a redox potential, or by stimulating the open/closed states from light irradiation.[11a-d] Because the DTE unit becomes a non-innocent ligand, the redox-state change may also have an influence on the closure/opening of the DTE unit.[12] More specifically, in bimetallic complexes in which a dithienylethene (DTE) linker connects two ruthenium carbon-rich units, closing at remarkably low voltage (0.4-0.5 V vs SCE) is achieved and give rise to multicolor electrochromism.[11e] This behavior could be transferred to self-assembled monolayers to reach dual responsive surfaces[11f] and exploited in the design of efficient multi-controllable molecular junctions in which both light and potential efficiently trigger the device response.[11g]

In this article, we extend this concept for the first time to the dual redox and optical control of chiroptical activity by (i) describing the synthesis of enantiopure complexes (**1o,c** and **2o,c**) consisting of ruthenium-bis-ethynyl complexes linked to helicene and DTE

units, and (ii) studying in details their behavior as chiroptical switches due to the reversible ring DTE closure/opening triggered by an electrical potential and by UV or visible lights. Indeed, since helicenes display strong chiroptical responses, they provide with tags that can be used for reading out the system, especially by electronic circular dichroism.

RESULTS

SYNTHESIS OF COMPLEXES 1o AND 2o

Two different systems were designed and are depicted in Chart 1. Molecule **1o** consists in a central *trans*-bis-ethynyl-Ru(η^2-dppe)$_2$ redox-active system (dppe:1,2-bis(diphenylphosphino)ethane) decorated on one side by an open photochromic DTE unit, and on the other side by an enantiopure carbo[6]helicene fragment. Molecule **2o** includes a central open photochromic DTE unit linked to two *trans*-bis-ethynyl-Ru(η^2-dppe)$_2$ moieties, each terminated by an enantiopure carbo[6]helicene fragment.

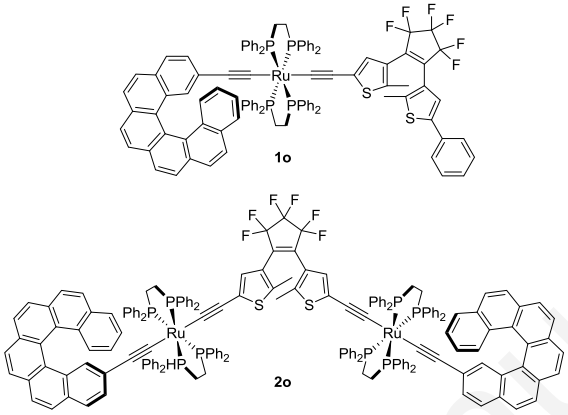

CHART 1. Chemical structure of the DTE based helicene-ethynyl-Ru switching systems (*P*-1o and (*P,P*)-2o enantiomers shown).

The strategies for synthesizing molecules **1o** and **2o** are described in Scheme 1. First, the 2-ethynyl[6]helicene ligand *rac*-, *P*- or *M*-**3**[6a] was reacted with the 16-electron precursor [Ru(η^2-dppe)$_2$Cl]OTf **4** in a degassed CH_2Cl_2 solution at 25 °C, yielding the cationic vinylidene complexes rac, *P*- or *M*-**5**, which was then reacted with mono-ethynyl DTE ligand **6o**[13] in the presence of $NaPF_6$ and NEt_3,[11d-h] to form respectively *rac*-, *P*- or *M*-**1o** as yellow solids, with overall yields between 73-84% (see Supplementary Information, SI). For the preparation of (*P*,*P*)- or (*M*,*M*)-**2o**, DTE-bis-ethynyl-bis-ruthenium complex **8o** was first obtained from the bis-ethynyl DTE **7o** according to a literature procedure,[11d,e] and was then reacted with 2 equivalents of *P*- or *M*-**3** under similar conditions as those used for **1o**. Enantiopure (*P*,*P*)- and (*M*,*M*)-**2o** were obtained as yellow solids with 58-69% overall yields. Note that only enantiopure **3** was used here in order to avoid the formation of the *meso* compound. All these species were fully characterized by means of ^{31}P, ^{1}H, and ^{13}C NMR spectroscopies and HR mass spectrometry. As an illustration, in the ^{1}H NMR spectrum of complex **1o**, the helicene protons are mostly deshielded with chemical shifts around 7.6-8 ppm. The typical two CH_3 groups from the DTE unit have distinct chemical shifts at 2.02 and 1.87 ppm. With ^{13}C NMR, the β-carbons from the two C≡C bonds display chemical shifts at 119.24 and 107.19 ppm. The CH_2 groups are diastereotopic owing to the presence of the chiral helicenic part, and were found as broad multiplets at 32.62 and 31.42 ppm. In the ^{31}P NMR spectrum, two signals were found at 54.44 and 51.38 ppm, respectively, as triplets (with a coupling constant of 23 Hz), again due to their diastereotopic relationship. In the ^{19}F NMR spectrum, each CF_2 groups from the DTE unit show a distinct signal. The NMR spectra of **2o** display the same general features, but are simplified due to a higher molecular symmetry (C_2 *vs.* C_1 for **1o**). For instance, the protons of the typical two methyl groups from the DTE unit resonate at 1.86 ppm (see SI).

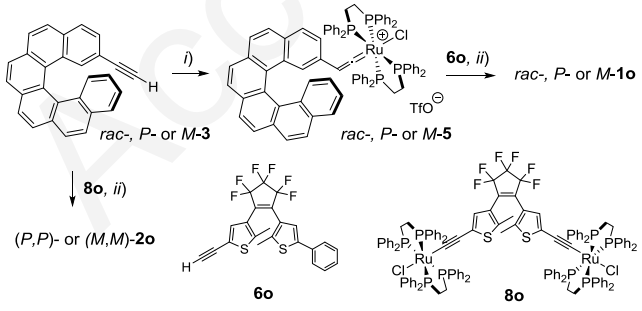

SCHEME 1 Synthesis of complex 1o and 2o. i) Ru(dppe)$_2$Cl]OTf (4), CH_2Cl_2, 25°C, 16 hrs, 87-96%; ii) NEt_3, CH_2Cl_2 $NaPF_6$, 25°C, 48-72 hrs, 82-96%; iii) 4, CH_2Cl_2, 25°C, 4 days; then NEt_3, CH_2Cl_2, 30 min, 58-69%.

Deep yellow single crystals of *rac*-**1o** were grown by diffusion of pentane vapors into a CH_2Cl_2 solution in the dark and the crystal structure was characterized by X-ray diffraction. Complex *rac*-**1o** crystallized in the centrosymmetric $P\bar{1}$ space group (Figure 1). From the structure, the ruthenium center displays a distorted octahedral geometry, with the two C≡C bonds in mutually *trans*-positions. Distortion along the C≡C bond of the helicene unit was observed. Indeed, compared with the angles along Ru−C≡C−DTE (Ru1−C81−C82 and C81−C82−C83) almost close to 180°, the angles along Ru−C≡C−[6]helicene show large deviations, especially the C1−C2−C3 angle being around 167°. This is probably caused by the steric hindrance between the [6]helicene unit and dppe ligands. The average number between the four angles of P−Ru1−C1 is 91.6°, which is larger than the average number 88.4° of P−Ru1−C81, indicating that the four P−Ru bonds diverge from the octahedral positions and slope slightly to the DTE side. Besides, the helicity (dihedral angle between two terminal helicene rings) of the helicene unit is 45.1°, and compares well with similar complexes.[6a] The dihedral angle between the two thiophenes from the DTE unit is 54.6° in the open form **1o** due to the steric hindrance from the two methyl groups. Finally, we also clearly found that although the compound crystallized in the racemic form, the stereochemistry of photoreactive anti-parallel open DTE unit is related with the stereochemistry of the helicene in the solid state: they show the same chirality in one molecule, *i.e*. when the chirality of helicene is *M*, the chirality of open DTE unit is also *M* (*vide infra*).

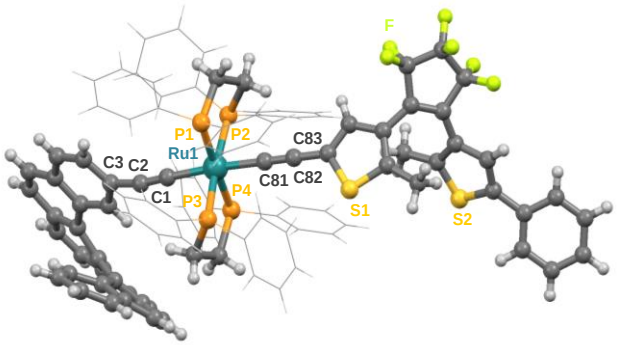

FIGURE 1. X-ray crystallographic structure of 1o (only *P* enantiomer is shown; the 8 phenyl groups from dppe ligands are shown in wireframe style for clarity).

SWITCHING ACTIVITY OF COMPLEX 1o/c

PHOTOCHROMIC PROPERTY

The light-triggered switching property of **1o** was studied first. Upon irradiation at 365 nm under a UV lamp, a yellow solution of the complex **1o** in the open state turned to the dark green close state complex **1c** (Scheme 2). Then, irradiating **1c** at 650 nm enabled to recover the starting yellow open state **1o**. The irradiation time varies, depending on the concentration and the power of the lamp. Note that the closed DTE unit generated two chiral centers at α-position of two thiophenes respectively, and because of photochemical electrocyclic reaction rule, conrotatory products were the only products, obtained with the two methyl groups in each side of the DTE plane, thus fixing the chirality of the α-carbon as either (*R*,*R*) or (*S*,*S*). Consequently, molecule **1c** can have two diastereomers (*P*,*R*,*R*)-**1c** (or (*M*,*S*,*S*)-**1c**) and (*P*,*S*,*S*)-**1c** (or (*M*,*R*,*R*)-**1c**). This photochemical closing process can be monitored by NMR spectroscopy. Indeed, upon UV light irradiation at 365 nm of a solution of **1o** (5×10^{-2} mol· L^{-1} in CD_2Cl_2) in an NMR tube, the conversion to **1c** monitored by ^{1}H NMR, revealed that the signals for the two DTE methyl groups at 2.02 and 1.87 ppm were decreasing and 4 signals at 2.19, 2.18, 2.16 and 2.15 ppm were increasing with the appearance of the two diastereomers in 1:1 ratio, thus showing no stereoselectivity in solution.[13] In addition, after sufficient irradiation, typically 30 minutes at this concentration, the **1o** signals have decreased to less than 2% (photostationary state, PSS), so that we can consider that **1o** can almost fully convert to **1c** under 365 nm. Similarly, **1c** turned back to **1o** with more than 98% of conversion after sufficient irradiation at 650 nm, although this process took 2 days due to high concentration. This result indicate that this light-triggered switching process occurs with full conversion.

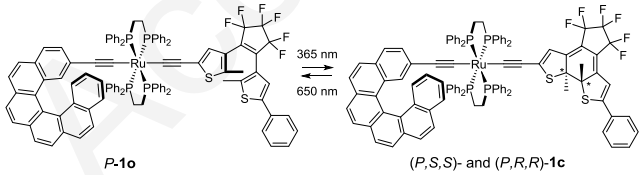

SCHEME 2. Reversible photochromic switching process between 1o and 1c.

The switching process was also investigated by UV-vis spectroscopy, by gradual irradiation at 365 nm of a CH_2Cl_2 solution (C 1 × 10^{-4} mol· L−1, Figure 2). Because of low concentration, the process only needed a few minutes.

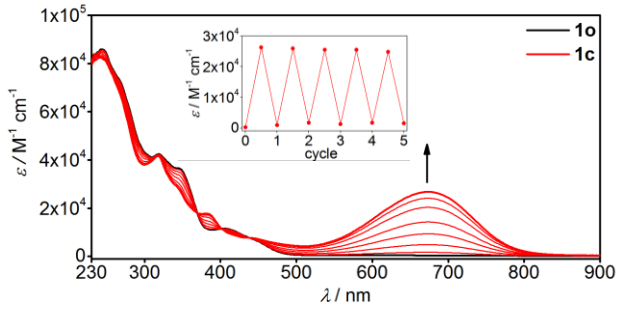

FIGURE 2. Up: Evolution of absorption spectra from 1o to 1c (PSS) by gradual irradiation at 365 nm. Insert: five switching cycles upon alternate irradiation at 365 nm and 650 nm.

The UV-vis spectrum of **1o** in CH_2Cl_2 exhibits a high energy band at 245 nm with $\varepsilon > 8 \times 10^4 \cdot M^{-1} \cdot cm^{-1}$, and longer wavelength shoulders at 318 and 347 nm. A band in the visible region at 406 nm with a shoulder at 445 nm and tailing down to 500 nm is also found and most probably corresponds to a MLCT type transition.[11d,e] Stepwise irradiation at 365 nm induced changes of several bands between 300 and 450 nm, with the one at 347 nm strongly decreasing, and with several isosbestic points, indicating that this process is unimolecular. Furthermore, a strong and broad absorption band at 679 nm with ε around 2.7×10^4 $M^{-1} \cdot cm^{-1}$ arose due to the π- π * transition of the closed conjugated DTE unit. Reversibility and repeatability of the process was then studied by irradiating successively the solution at 365 nm and 650 nm and monitoring the absorption at 679 nm. A total of 5 cycles were performed with high reversibility (Figure 2 insert). In conclusion, **1o/c** shows efficient light-triggered switching activity with the usual good contrast in the visible range (ε values from 0 to 2.7×10^4 $M^{-1} \cdot cm^{-1}$ at 679 nm).

The photoresponsive activity was also followed by ECD spectroscopy. The ECD spectrum of *P*-**1o** (Figure 3) displays three strong negative bands at 247, 278 nm and 303 nm ($\Delta\varepsilon$ = -178, -81, -27 $M^{-1} \cdot cm^{-1}$, respectively), strong positive bands at 335 nm and 351 nm ($\Delta\varepsilon$ = + 88 and 101 $M^{-1} \cdot cm^{-1}$, respectively)

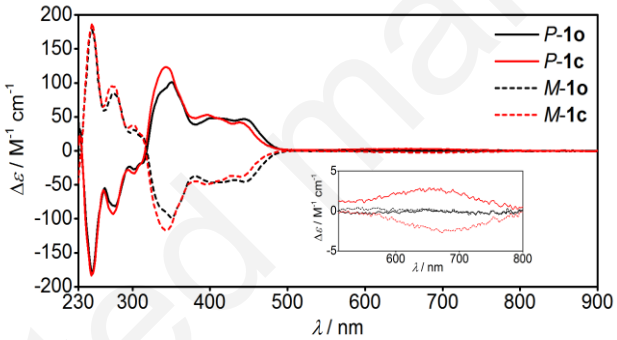

FIGURE 3. ECD spectra of the open state *P*- and *M*-1o, and of the closed state *P*- and *M*-1c in CH_2Cl_2 (C 1×10^{-4} $mol^{-1} \cdot L^{-1}$). Insert: zoom between 500-700 nm.

and additional positive bands in the lower energy region at 403 nm ($\Delta\varepsilon$ = +48 $M^{-1} \cdot cm^{-1}$) and 445 nm ($\Delta\varepsilon$ = +46 $L \cdot mol^{-1} \cdot cm^{-1}$) with a tail down to 500 nm. Note that the sign of these two bands agrees well with its starting ligand *P*-**3**, thus enabling to confirm the *P*-(+) [and *M*-(-)] absolute configuration.

Upon irradiation at 365 nm for a few minutes, *P*-**1o** could be completely converted into *P*-**1c**, which showed similar ECD-active bands, but with slight changes in their intensities, the strongest change being found at 343 nm with an increase from +92 to +122 $M^{-1} \cdot cm^{-1}$ ($\Delta(\Delta\varepsilon)$ = 30 $M^{-1} \cdot cm^{-1}$). These results indicate that the ring closure in the DTE unit has an influence on the strong ECD-active bands of the molecule. In addition, the absorption band at 679 nm appears to be slightly ECD-active, with $\Delta\varepsilon$ small around +3 $L \cdot mol^{-1} \cdot cm^{-1}$ for *P*-**1c** enantiomer. Although the signal is small, it corresponds to an induced circular dichroism since the ring closure is not stereoselective, and this illustrates that the chirality of the helicene can influence the DTE response through the ruthenium bridge, thus suggesting a strong electronic communication between each part of the molecule.[9,11] In summary, these results show that the chiroptical properties of carbon-rich helicenic DTE-Ru conjugate **1o/c** can be efficiently tuned by the photochromic DTE ring closure/opening process thus leading to an efficient chiroptical ligh-triggered switching activity.[5,6]

REDOX ACTIVITY OF COMPLEX 1o/c

CYCLIC VOLTAMMETRY

The redox-triggered switching process was also investigated. First, both the open state **1o** and the closed state **1c** were studied by cyclic voltammetry (CV). The CV measurements were performed in CH_2Cl_2 solutions in the dark and under inert atmosphere. NBu_4PF_6 was used as the supporting electrolyte (C = 0.2 mol·L^{-1}). The open state **1o** shows a reversible oxidation wave with $E°_{[\mathbf{1o}]^{\cdot+}/\mathbf{1o}}$ = +0.45 V (*vs.* SCE, thereafter), and an irreversible oxidation wave with $E^{pa}_{[\mathbf{1o}]^{2+}/[\mathbf{1o}]^{\cdot+}}$ = +1.31 V at 0.2 V·s^{-1} (Figures 4a,b), reminiscent of the usual behavior observed for monometallic DTE complexes in their open state.[11f] The close system **1c** shows three distinct oxidation waves, with the two first waves being chemically reversible with $E°_{[\mathbf{1c}]^{\cdot+}/\mathbf{1c}}$ = +0.36 V and $E°_{[\mathbf{1c}]^{2+}/[\mathbf{1c}]^{\cdot+}}$ = +0.80 V (*vs.* SCE), whereas the third oxidation wave exhibits partial chemical reversibility at high scanning rate only (Figure 4c-e). The first wave is assigned to the oxidation of the ruthenium carbon-rich system bearing the conjugated closed DTE and helicene units,[11d,e] whereas the exact origin of the second and third processes probably involving the conjugated ligands remain unclear so far. Based on these results, it appeared interesting to take advantage of the first reversible oxidation processes of both **1o** and **1c** and to examine their electrochromic activity.

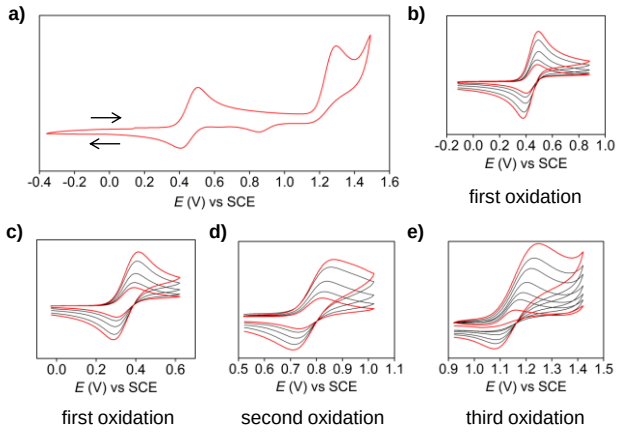

FIGURE 4. a) Full cyclic voltammograms of 1o at scanning rate of 0.2 V·s^{-1}; b) First oxidation wave of 1o at scanning rates from 0.06 V·s^{-1} to 0.6 V·s^{-1} ; c-e) cyclic voltammograms of each oxidation wave of 1c with different scan-rates: c) first oxidation with scan-rates from 0.06 V·s^{-1} to 0.6 V·s^{-1}; d) second oxidation with scan-rates from 0.06 V·s^{-1} to 0.6 V·s^{-1}; e) third oxidation with scan-rates from 0.06 V·s^{-1} to 2 V·s^{-1}.

The first oxidation process of the open form **1o** was therefore investigated by spectroelectrochemistry in the UV-Vis-NIR region. The measurements were performed in an optically transparent thin-layer electrochemical (OTTLE) cell at 25 °C using 1,2-dichloroethane as the solvent (0.2 mol·L^{-1} of NBu_4PF_6 as the electrolyte and Ag wire as the pseudo-reference electrode). The evolution of the oxidation process was recorded stepwise by gradual increase of the potential from −0.2 V to +0.6 V *vs*. Ag wire (Figure 5). The **1o** → [**1o**]$^{\cdot+}$ process showed several changes in the 250-600 nm range with the presence of several isosbestic points. In addition, a strong band in the NIR region appeared, centered at 1272 nm with ε around 2.3 × 10^4 M^{-1}·cm^{-1}. Such NIR feature is typically observed in ruthenium bis(acetylide) oxidized complexes.[10] The **1o** → [**1o**]$^{\cdot+}$ process was also examined by ECD spectroscopy which revealed significant changes in *P*-[**1o**]$^{\cdot+}$ as compared to the starting *P*-**1o**. For instance, the strong positive band at 351 nm was red-shifted to 360 nm while the positive ones between 400-500 nm underwent a strong decrease in their intensities (typically from $\Delta\varepsilon$ = +47 to +17 M^{-1}·cm^{-1} at 450 nm *i.e.* $\Delta(\Delta\varepsilon)$ = -30 M^{-1}·cm^{-1}). Besides, a new band appeared at 525 nm ($\Delta\varepsilon$= +8 M^{-1}·cm^{-1}) with a tail down to 560 nm. These results indicate that the redox-triggered switching process is as efficient as the light-triggered switching process when considering the modulation of the ECD spectra. Note, however, that the NIR band centered on the central metal-carbon-rich part in [**1o**]$^{\cdot+}$ is not ECD-active.

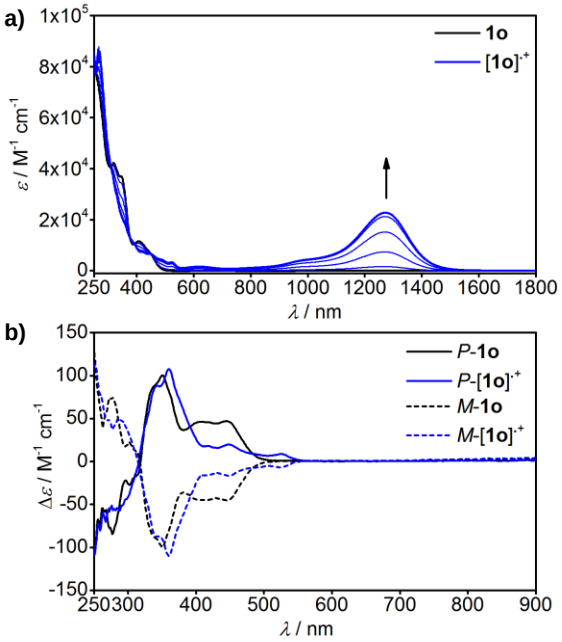

FIGURE 5. a) Evolution of absorption spectra from 1o to $[1o]^{\bullet+}$. b) ECD spectra of the open state *P*- and *M*-1o and of the open oxidized state *P*- and *M*-$[1o]^{\bullet+}$.

The electrochromic activity of **1c** was also studied; the first oxidation process was followed upon gradual increase of the potential from −0.2 V to +0.6 V *vs*. Ag wire (Figure 6). Interestingly, the spectroelectrochemistry revealed an unanticipated result since two stages are appearing in this oxidation process. At the beginning (first stage) of the oxidation, the visible band at 679 nm regularly decreased with its maximum shifting hypsochromically from 679 nm to 657 nm. Meanwhile, a new broad band was generated at 965 nm with tails further than 1800 nm out of the measurement window. As a result, two distinct isobestic points at 543 nm and 778 nm were observed. A strong positive current was detected, indicating that there was an oxidation process occurring during these observations. Then, (second stage), a broad signal peak at 1272 nm started to be generated, while the signal at 965 nm started to decrease; at this stage, no current production was detected anymore. Finally, this process stopped when the band at 1272 nm reached its maximum around 2×10^4 $M^{-1} \cdot cm^{-1}$, and the bands at 657 nm and 964 nm almost disappeared. From the changes of spectra and current responses, one can conclude that the second step was not directly induced by electrochemical oxidation. Besides, the final spectrum was found to be very similar to the spectrum of $[\mathbf{1o}]^{\bullet+}$ with the same absorption band at 1272 nm. Thus, these observations indicate that the two steps should correspond to the oxidation step that generates $[\mathbf{1c}]^{\bullet+}$ from **1c** with two signals at 657 nm and 964 nm, followed by the ring opening isomerization of $[\mathbf{1c}]^{\bullet+}$ to $[\mathbf{1o}]^{\bullet+}$. As **1c** is easier to oxidize than **1o**, each produced $[\mathbf{1o}]^{\bullet+}$ species can oxidize another molecule of **1c** to lead to another ring opening and so on. This process thus is an electrocatalytic process, ,[12] observed for the first time with ruthenium complex/DTE adducts. Indeed, a final reduction enabled to go back to the open form **1o** while another irradiation of **1o** at 365 nm regenerated the closed form **1c** again. All these steps (1 to 4) are summarized on Figure 7.

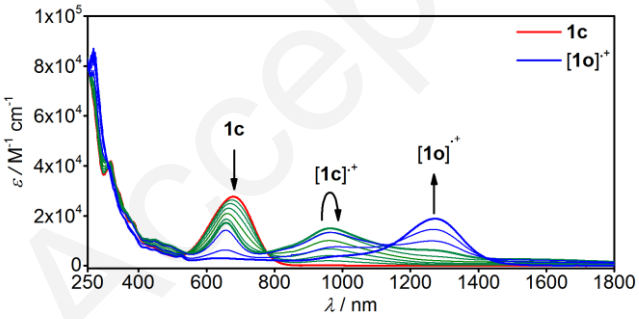

FIGURE 6. Evolution of absorption spectra during the oxidation process 1c → $[1c]^{\bullet+}$ → $[1o]^{\bullet+}$.

"NOR" LOGIC GATE

As a result, a three-state cycling process (Figure 8a) can be performed starting from **1o**: *i*) irradiation at 365 nm generates **1c**; *ii*) oxidizing **1c** forms $[\mathbf{1o}]^{\bullet+}$ at +0.6 V (vs. Ag wire); *iii*) reducing $[\mathbf{1o}]^{\bullet+}$ leads back to **1o** at −0.4 V (vs. Ag wire). A total of 5 full cycles could be performed, and by reading ε values at 679 nm and at 1272 nm. It was found that at 679 nm the signal shows

OFF→ON→OFF, while at 1272 nm the signal shows OFF→OFF→ON responses (Figure 8b). Note that after 5 cycles around 50% of degradation in our conditions was observed, probably due to partial degradation of the oxidized radical species during the process. Besides, based on this unique photochromic and electrochromic property, this molecule can be treated as an optical logic gate at 679 nm.[14] One may define that the open state **1o** with low absorption at 679 nm as "0", and closed state **1c** with high absorption at 679 nm as "1". The output can be measured by UV-vis absorption. Starting from **1c**, two inputs can be applied: irradiation at 650 nm (hν) and external potential at +0.6 V, then −0.4 V *vs*. Ag wire (E). These two inputs can be defined as either "0" and "1". Either irradiation (1,0) or external potential (0,1) or together (1,1) can trigger the ring opening reaction of **1c** and form the low absorption species **1o** (output 0). So, we can treat this process as an "NOR" logic gate (Figure 8c).[14]

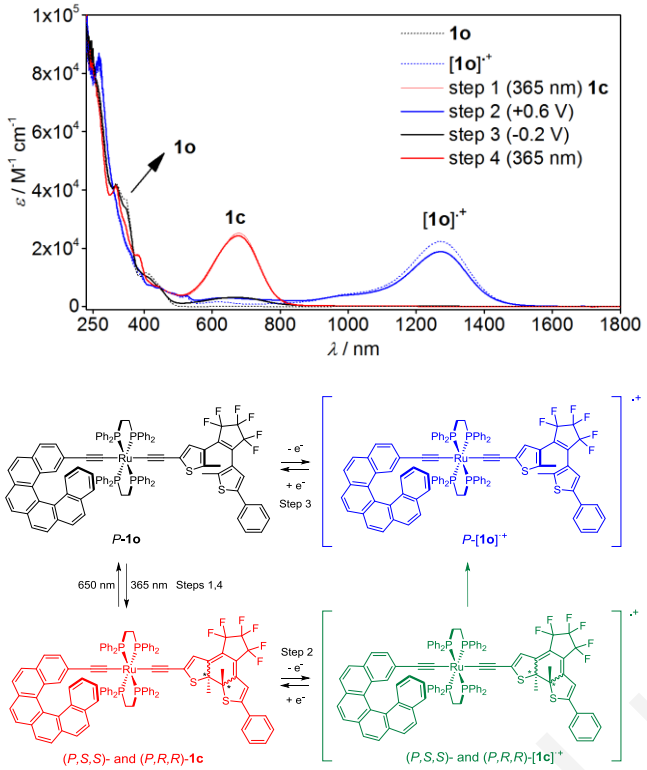

FIGURE 7. The photochromic and electrochromic steps of cycle 1o → 1c → $[1c]^{\cdot+}$ (reactive) → $[1o]^{\cdot+}$ → 1o.

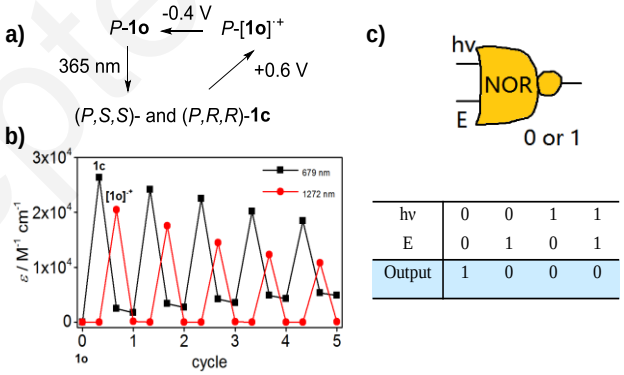

hν	0	0	1	1
E	0	1	0	1
Output	1	0	0	0

FIGURE 8. a) Three-state cycle obtained from the 1o/1c system upon light and redox stimuli; b) Five switching cycles between 1o → 1c → $[1o]^{\cdot+}$ at 679 nm (black) and 1272 nm (red); c) symbol and truth table of the "NOR" logic gate.

In summary, the mono-helicenic-ruthenium DTE conjugate **1o**/**c** undergoes easy redox-triggered cycloreversion, *i.e. ring opening* of the closed form **1c** upon oxidation. In comparison, systems from the literature[11c] display one DTE unit and two -Ru- arylethynyle- centers and all show redox-triggered *ring closure* of the DTE units upon oxidation, a particular case that we also applied to the chiroptical system.

PHOTOCHEMICAL SWITCHING ACTIVITY OF 2o

Complex **2o** displayed similar photochromic behavior as **1o** and could be transformed to the closed state **2c** upon irradiation at 365 nm and recovered back to the open state **2o** by irradiation at 650 nm. Like **1c**, **2c** was also generated as a pair of diastereoisomers due to the newly formed chiral center at αpositions of the two thiophenes. The conrotatory ring closing reaction can generate both (*R*,*R*) and (*S*,*S*) configurations and thus generate a pair of diastereomers (*P*,*P*,*R*,*R*)- and (*P*,*P*,*S*,*S*)-**2c** when starting from the enantiopure (*P*,*P*)-**2o** (Scheme 3). The photochemical process was followed by UV-vis spectroscopy. Complex **2o** shows similar UV-vis spectrum as **1o** but with stronger intensity, and displayed a strong band at 244 nm ($\varepsilon > 1.4 \times 10^5$ $M^{-1}\cdot cm^{-1}$), two moderate ones at 323 and 349 nm ($\varepsilon \sim 7 \times 10^4$ $M^{-1}\cdot cm^{-1}$) and another band in the visible region at 406 nm with a shoulder at 450 nm and tailing down to 500 nm (MLCT, $\varepsilon \sim 1.4 \times 10^4$ $M^{-1}\cdot cm^{-1}$ at 450 nm). Upon step-wise irradiation to **2c**, the yellow solution turned to very deep dark green. Several isobestic points were observed in the UV-vis spectrum, with a strong decrease of the signal at 349 nm and two new bands appearing at longer wavelengths at 665 and 720 nm (ε 3.8×10^4 $M^{-1}\cdot cm^{-1}$) due to the greater π-extended conjugation of the closed DTE unit. The presence of several transitions in this range is typical of DTE bearing two ruthenium bis(acetylide) moieties displaying several conformers.[11e] This process was also studied by NMR spectroscopy and full conversion was verified together with the formation of two diastereoisomers in a 1:1 ratio as demonstrated for instance by ^1H and ^{19}F NMR spectroscopies (see SI).

.

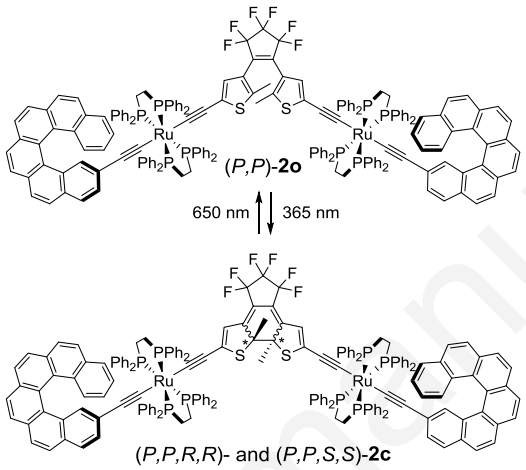

SCHEME 3. Photochromic switching between 2o and 2c ((*P,P*) enantiomers).

(*P*,*P*)-**2o** shows quite similar ECD spectrum as *P*-**1o**, but with intensities twice as large for most of the signals indicating that these ECD signals are mainly contributing from the helicene-ruthenium parts with almost no electronic communication between these two parts through the open DTE bridge. When **2o** is transformed into **2c** upon irradiation at 365 nm, the ECD-active band centered at 350 nm increased while the band at 445 nm decreased. Notably, a weak band around 679 nm with a $\Delta\varepsilon$ value of +6 $L\cdot mol^{-1}\cdot cm^{-1}$ was also observed and indicated an induced ECD response from the helicene parts to the DTE chromophore.

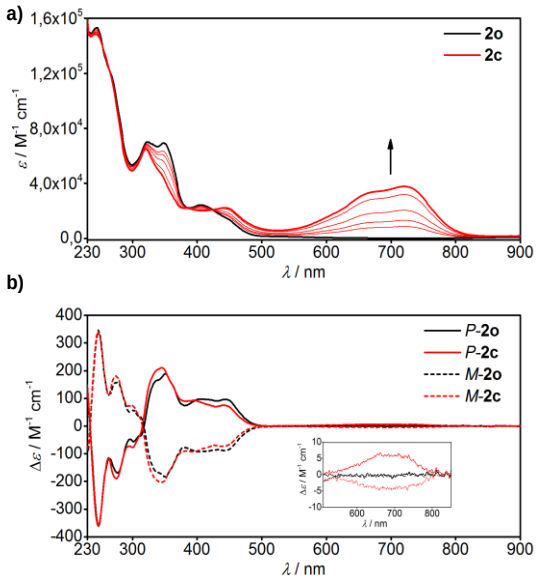

FIGURE 9. a) Evolution of absorption spectra from 2o to 2c by gradual irradiation at 365 nm. b) ECD spectra of the open neutral state (*P,P*)-2o, (*M,M*)-2o, the closed neutral state (*P,P,R,R*)- and (*P,P,S,S*)-2c and (*M,M,S,S*)- and (*M,M,R,R*)-2c. Insert: zoom between 500-850 nm.

REDOX ACTIVITY OF COMPLEX 2o/c

CYCLIC VOLTAMMETRY

The cyclic voltammetry for both **2o** and **2c** was first examined. The CV measurements were performed in CH_2Cl_2 solution in the dark and under inert atmosphere (0.2 mol·L^{-1} NBu_4PF_6 as the supporting electrolyte). The open state **2o** presents an almost reversible broad redox system at 0.43 V *vs*. SCE which is composed of two close one-electron oxidation processes corresponding to the two electronically independent ruthenium carbon rich systems and leading to [**2o**]$^{2+}$ as previously observed for parents complexes.[11d,e] Notably, both the DTE unit and the helicenes ligands are non-innocent ligands and contribute to the oxidation process. For the closed state **2c**, two reversible monoelectronic oxidation waves with close potential values were found with $E°_{\mathbf{2c}^{\cdot+}/\mathbf{2c}}$ = +0.10 V and $E°_{\mathbf{2c}^{2+}/\mathbf{2c}^{\cdot+}}$ = +0.21 V (see SI). This result shows that the two halves of the complex are no longer independent because of the electronic communication through the closed conjugated DTE bridge.[9]

ELECTROCHROMIC ACTIVITY

Spectroelectrochemical studies in the UV-vis-NIR region was then performed of the open form **2o** in 1,2-dichloroethane with NBu_4PF_6 as the supporting electrolyte in the OTTLE cell well-protected from air and light. The evolution curves of the two-electrons oxidation process **2o** → [**2o**]$^{2+}$ were recorded by stepwise increase of potential from −0.6 V to +0.7 V (*vs*. Ag wire pseudo-reference electrode). The results indicated the expected multi-step process (Figure 10): a strong and broad new band appeared between 600 and 1100 nm, centered at 825 nm with ε = 2.2 × 10^4 L·mol^{-1}·cm^{-1}, while a band in the low energy domain at 1268 nm firstly appeared and then decreased, indicating that isomerization occurred.[11d,e] Indeed, reduction of this oxidized species by applying a potential of −0.6 V, no longer yielded **2o**, but **2c** with almost full conversion, as illustrated by the strong bands at 665 and 720 nm characteristic of **2c** in the UV-visible spectrum. Then, we could observe that further photo irradiation at 650 nm fully regenerated complex **2o**.

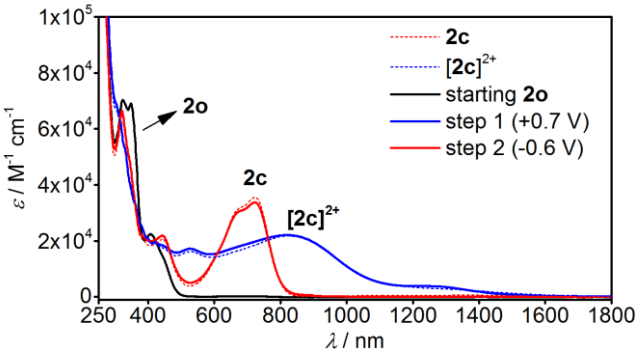

FIGURE 10. The electrochromic steps of cycle 2o → [2o]$^{2+}$ (not observed) → [2c]$^{2+}$ → 2c.

To further explore the isomerization from [**2o**]$^{2+}$ to [**2c**]$^{2+}$, we also studied the electrochromic property of the closed state **2c**. Complex **2c** shows progressive transformation to the first oxidized state [**2c**]$^{\cdot+}$ upon oxidation (Figure 11a), then to the second oxidized state [**2c**]$^{2+}$ (Figure 11c) with several identical isosbestic points. In the first oxidation of **2c**, the strong bands at 665 and 720 nm decreased and two new strong bands appeared at 1125 and 1355 nm with a tail longer than 1800 nm. In the second oxidation process, these two bands decreased, and a new band centered at 825 nm formed, indicating the formation of [**2c**]$^{2+}$. This spectrum is very similar to the one coming from the oxidation of **2o**. Furthermore, the reduction process of [**2c**]$^{2+}$ leads back to **2c**. From these results, one can conclude that the redox process from **2c** to [**2c**]$^{2+}$ is reversible with an intermediate [**2c**]$^{\cdot+}$, while the redox process of **2o** is irreversible with the isomerization in the oxidation process from [**2o**]$^{2+}$ to [**2c**]$^{2+}$. These result are in line with previous observations from parent complexes.[11d,e]

Reversible evolution of **2c** → [**2c**]$^{\cdot+}$ → [**2c**]$^{2+}$ was also monitored by ECD spectroelectrochemistry (Figures 11b,d,e,f). For (*P*,*P*)-**2c** → (*P*,*P*)-[**2c**]$^{\cdot+}$, large changes were found between 300 to 500 nm with several isosbestic points. The most interesting change occurred in the lower energy region. Indeed, (*P*,*P*)-**2c** showed an ECD-active band at 679 nm with $\Delta\varepsilon$ = +6 L·mol^{-1}·cm^{-1}. Upon oxidation to (*P*,*P*)-[**2c**]$^{\cdot+}$, this band shifted to 700 nm and decreased in intensity to +4 L·mol^{-1}·cm^{-1} (Figure 11e) . Upon further oxidation to (*P*,*P*)-[**2c**]$^{2+}$, this band became bisignate with positive sign at 625 nm ($\Delta\varepsilon$ = +8 L·mol^{-1}·cm^{-1}) and negative sign at 800 nm ($\Delta\varepsilon$ = -6 L·mol^{-1}·cm^{-1}) (Figure 11f).

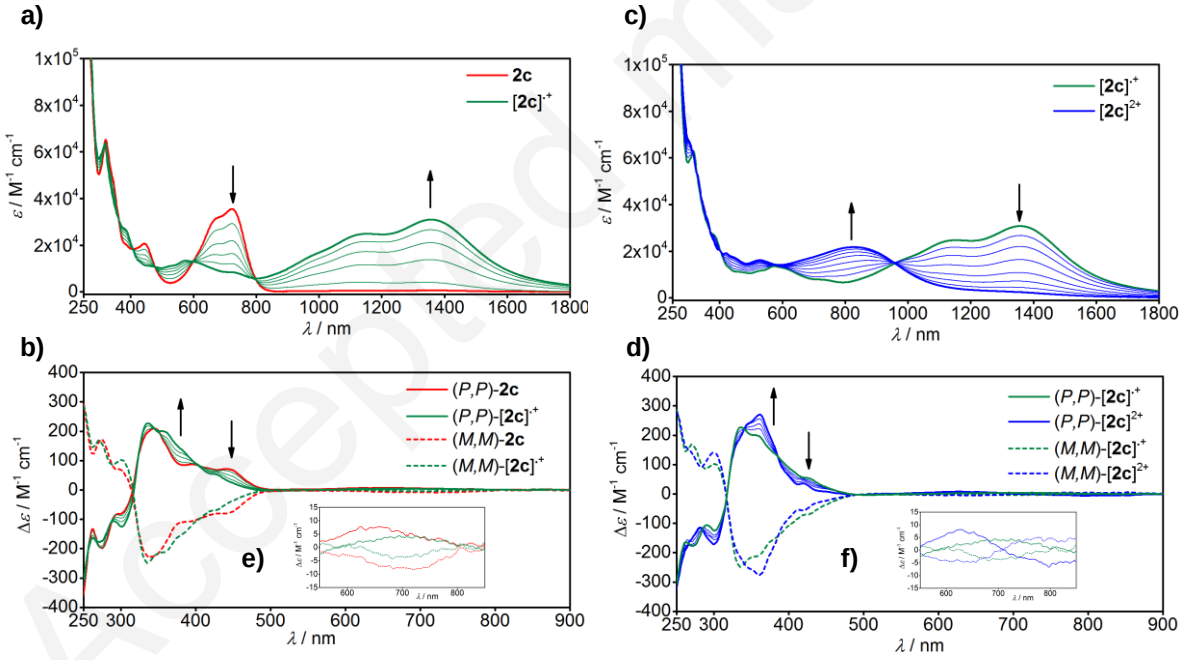

FIGURE 11. Absorption changes in the UV-vis-NIR range observed upon oxidative transformations 2c → [2c]$^{\cdot+}$ (11a) and [2c]$^{\cdot+}$ → [2c]$^{2+}$ (11c) and their corresponding spectroelectrochemical ECD spectra of the (*P*,*P*) and (*M*,*M*) enantiomers (11b,d,e,f).

Finally, the oxidation process of **2o** was also examined, and, as expected, the oxidation ended-up with the spectrum of [**2c**]$^{2+}$, which is another proof of the isomerization from [**2o**]$^{2+}$ to [**2c**]$^{2+}$ (see Figure 12).

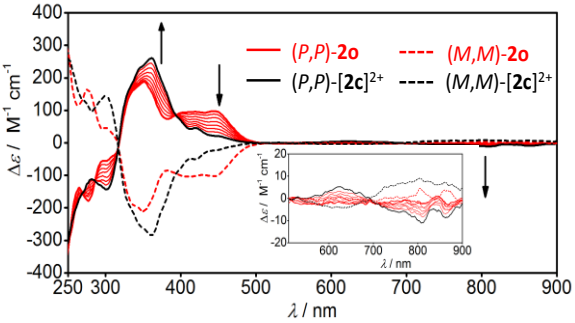

Figure 12. ECD spectra of the open neutral state (*P,P*)- and (*M,M*)-2o and their evolution upon oxidation to (*P,P*)- and (*M,M*)-[2c]$^{2+}$. Insert: zoom between 500-900 nm.

"OR" LOGIC GATE

Based on its photochromic and electrochromic properties, complex **2o,c** can also be used as a logic gate.[14] For example, we can use the absorption (ε) or the circular dichroism ($\Delta\varepsilon$) of this molecule at 679 nm as outputs. The absence of absorption nor CD signal defines "0", a high absorption or CD signal, defines "1". Two inputs can be also defined: irradiation at 365 nm corresponds to "1" in the photochemical process, otherwise "0" corresponds to no irradiation. External redox potential of +0.7 V then of −0.6 V *vs*. Ag wire corresponds to "1" in E, otherwise "0" corresponds to the absence of redox stimulus. In this logic gate, when there is no irradiation nor potential (0, 0), the open state **2o** can keep its open form, so the output is still "0". However, when there is either irradiation (1,0) or the external potential (0,1) or both (1,1), the open state **2o** will transform to the closed state **2c,** the output will then be "1". As a result, the system can be described as an "OR" logic gate (Figure 13).[14]

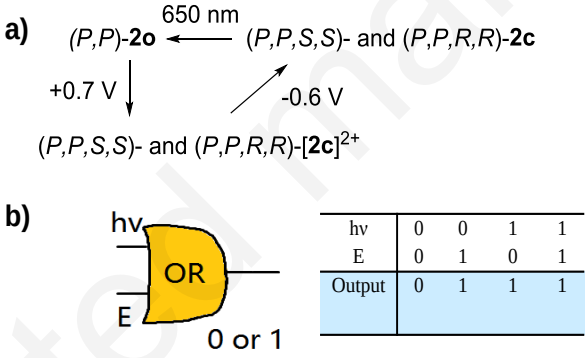

Figure 13. a) Three-state cycle obtained from the 2o/2c system upon light and redox stimuli; b) The symbol of "OR" logic gate and its truth table.

CONCLUSION

In conclusion, we have synthesized enantiomerically enriched mono- and bis-([6]helicene-≡-Ru(dppe)$_2$-≡)-DTE complexes **1o,c** and **2o**,**c**. Both the photochromic and electrochromic properties were studied and attractive isomerization processes were observed, *i.e.* ring opening from closed oxidized state to open oxidized in the case of the mono-substituted helicene-alkynyl-Ru complex **1o**,**c**, and ring closure from open oxidized state to closed oxidized in the case of the bis-substituted helicene-alkynyl-Ru complex **2o**,**c**. These properties make these complexes new types of molecular "NOR"/"OR" logic gates with output being both absorption or the circular dichroism signal. These systems also appeared as new types of light- and redox-triggered organometallic chiroptical switches.[6,15]

ASSOCIATED CONTENT

Supporting Information

The Supporting Information is available free of charge on the ACS Publications website: experimental procedures for **1o,c** and **2o,c**, NMR and X-ray data. Cif and checkcif files of **1o**.

AUTHOR INFORMATION

Corresponding Author

Email: stephane.rigaut@univ-rennes1.fr, jeanne.crassous@univ-rennes1.fr

ORCID

Jeanne Crassous: 0000-0002-4037-6067

Stéphane Rigaut: 0000-0001-7001-9039

Lucie Norel : 0000-0001-6654-1211

Notes

The authors declare no competing financial interest.

ACKNOWLEDGMENT

We thank the Ministère de l'Education Nationale, de la Recherche et de la Technologie, the Centre National de la Recherche Scientifique (CNRS), University of Rennes 1, and the ANR (12-BS07-0004-METALHEL-01).

REFERENCES

(1) a) Martin, R. H. *Angew. Chem., Int. Ed.* **1974**, *13*, 649-660; b) Katz, T. J. *Angew. Chem. Int. Ed.* **2000**, *39*, 1921-1923; c) Urbano, A. *Angew. Chem. Int. Ed.* **2003**, *42*, 3986-3989; d) Rajca, A.; Miyasaka, M. in: Müller, T. J. J.; Bunz U.H. F. (Eds.), *Functional Organic Materials*, Wiley-VCH Verlag GmbH & Co. KGaA, **2007**, p. 547; e) Dumitrascu, F.; Dumitrescu, D. G.; Aron, I. *Arkivoc* **2010**, *1*, 1-32; f) Stara, I. G.; Stary, I. in: Siegel, J. S.; Tobe Y. (Eds.), *Science of Synthesis*, Thieme, Stuttgart, **2010**, *45*, p. 885; g) Shen, Y.; Chen, C. -F. *Chem. Rev.* **2011**, *112*, 1463-1535; h) Gingras, M. *Chem. Soc. Rev.* **2013**, *42*, 968-1006; i) Saleh, N.; Shen, C.; Crassous, J. *Chem. Sci.* **2014**, *5*, 3680-3694**;** j) Bosson, J.; Gouin, J.; Lacour, J. *Chem. Soc. Rev.* **2014**, *43*, 2824-2840; k) Aillard, P.; Voituriez, A.; Marinetti, A. *Dalton Trans.* **2014**, *43*, 15263-15278.

(2) a) Furche, F.; Ahlrichs, R.; Wachsmann, C.; Weber, E.; Sobanski, A.; Vögtle, F.; Grimme, S. *J. Am. Chem. Soc.* **2000**, *122*, 1717-1724; b) Autschbach, J. Chirality **2009**, *21*, E116.

(3) a) Riehl, J. P.; Muller, G. in: N. Berova, P. L. Polavarapu, K. Nakanishi, R. W. Woody (Eds.), *Comprehensive Chiroptical Spectroscopy*, vol. 1, John Wiley & Sons, Inc., **2012**, p. 65; b) Maeda, H.; Bando, Y. *Pure Appl. Chem.* **2013**, *85*, 1967-1978; c) Sanchez-Carnerero, E. M.; Agarrabeitia, A. R.; Moreno, F.; Maroto, B. L.; Muller, G.; Ortiz, M. J.; de la Moya, S. *Chem. Eur. J.* **2015**, *21*, 1-14

(4) a) Amabilino D. (Ed.), *Chirality at the Nanoscale, Nanoparticles, Surfaces, Materials and more*, Wiley-VCH, **2009**; b) B. L. Feringa, W.R. Browne, Molecular Switches, 2nd edition, Wiley-VCH, 2011; c) V. Balzani, A. Credi, M. Venturi (Eds.), *Molecular Devices and Machines. Concepts and Perspectives for the Nanoworld*, Wiley-VCH, Weinheim, **2008**.

(5) a) Canary, J. W.; Mortezaei, S.; Liang, J. *Coord. Chem. Rev.* **2010**, *254*, 2249-2266; b) Miyake, H.; Tsukube, H. *Chem. Soc. Rev.* **2012**, *41*, 6977-6991; c) Crassous, J. *Chem. Comm.* **2012**, 48, 9687-9695; d) Dai, Z.; Lee, J.; Zhang, W. *Molecules*, **2012**, *17*, 1247-1277.

(6) a) Anger, E.; Srebro, M.; Vanthuyne, N.; Toupet, L.; Rigaut, S.; Roussel, C.; Autschbach, J.; Crassous, J.; Réau, R. J. Am. Chem. Soc. 2012, 134, 15628-15631; b) Biet, T.; Fihey, A.; Cauchy, T.; Vanthuyne, N.; Roussel, C.; Crassous J., Avarvari, N. *Chem. Eur. J.* **2013**, *19*, 13160-13167; c) Anger, E.; Srebro, M.; Vanthuyne, N.; Roussel, C.; Toupet, L.; Autschbach, J.; Réau, R.; Crassous. J. *Chem. Comm.* **2014**, *50*, 2854; c) Schweinfurth, D.; Zalibera, M.; Kathan, M.; Shen, C.; Mazzolini, M.; Trapp, N.; Crassous, J.; Gescheidt, G.; Diederich, F. *J. Am. Chem. Soc.* **2014**, *136*, 13045-13052; d) Srebro, M.; Anger, E.; Moore, II, B.; Vanthuyne, N.; Roussel, C.; Réau, R.; Autschbach, J.; Crassous, J. *Chem. Eur. J.* **2015**, *21*, 17100-17115; d) Saleh, N.; Moore, II, B.; Srebro, M.; Vanthuyne, N.; Toupet, L.; Williams, J. A. G.; Roussel, C.; Deol, K. K.; Muller, G.; Autschbach, J.; Crassous, J. *Chem. Eur. J.* **2015**, *21*, 1673-1681; e) Shen, C.; Loas, G.; Srebro-Hooper, M.; Vanthuyne, N.; Toupet, L.; Cador, O.; Paul, F.; López Navarrete, J. T.; Ramírez, F. J.; Nieto-Ortega, B.; Casado, J.; Autschbach, J.; Vallet, M.; J. Crassous, *Angew. Chem. Int. Ed.* **2016**, *55*, 8062-8066; f) Isla, H.; Srebro-Hooper,* M.; Jean, M.; Vanthuyne, N.; Roisnel, T.; Lunkley, J. L.; Muller, G.; Williams, J. A. G.; Autschbach, J.; Crassous, J. *Chem. Comm.* **2016**, *52*, 5932-5935; g) For a review on helicene-based chiroptical switches see: Isla, H.; Crassous, J.*Comptes Rendus Chimie* **2016**, *19*, 39-49.

(7) a) Irie, M. *Chem. Rev.* **2000**, *100*, 1685-1716; b) Irie, M.; Fukaminato, T.; Matsuda, K.; Kobatake, S. *Chem. Rev.* **2014**, *114*, 12174-12277.

(8) a) Dinescu, L.; Wang, Z. Y. *Chem. Commun.* **1999**, 2497-2498; b) Norsten, T. B.; Peters, A.; McDonald, R.; Wang, M.; Branda, N. R. *J. Am. Chem. Soc.* **2001**, *123*, 7447-7448; c) Wigglesworth, T. J.; Sud, D.; Norsten, T. B.; Lekhi, V. S.; Branda, N. R. *J. Am. Chem. Soc.* **2005**,

127, 7272-7273; d) Okuyama, T.; Tani, Y.; Miyake, K.; Yokoyama, Y. *J. Org. Chem.* **2007**, *72*, 1634-1638; e) Tani, Y.; Ubukata, T.; Yokoyama, Y.; Yokoyama, Y. *J. Org. Chem.* **2007**, *72*, 1639-1644.
(9) (a) Aguirre-Etcheverry, P.; O Hare, D. *Chem. Rev.* **2010**, *110*, 4839-4864; b) Costuas, K.; Rigaut, S. *Dalton T.* **2011**, *40*, 5643-5658; c) Low, P. J. *Coord. Chem. Rev.* **2013,** *257*, 1507-1532.
(10) a) Di Piazza, E.; Norel, L.; Costuas, K.; Bourdolle, A.; Maury, O.; Rigaut S. *J. Am. Chem. Soc.* **2011**, *133*, 6174-6176; b) Norel, L; Di Piazza, E.; Feng, M. A.; Vacher, A.; He, X.; Roisnel, T.; Maury, O.; Rigaut, S. *Organometallics* **2014**, *33*, 4824-4835; c) Samoc, M.; Gauthier, N.; Cifuentes, M. P.; Paul, F.; Lapinte C.; Humphrey, M. G. *Angew. Chem. Int. Ed.*, **2006**, *45*, 7376-7379; d) Norel, L.; Min, F.; Bernot, K.; Roisnel, T.; Guizouarn, T.; Costuas, K.; Rigaut, S. *Inorg. Chem.* **2014**, *53*, 2361-2363; e) Mahapatro, A. K.; Ying, J.; Ren, T. ;and Janes, D. B. *Nano Lett.*, **2008**, 8, 2131-2136; f) Burgun, A.; Gendron, F.; Sumby, C. J.; Roisnel, T.; Cador, O.; Costuas, K.; Halet, J.-F.; Bruce, M. I.; Lapinte, C. *Organometallics* **2014**, *33*, 2613-2627; g) Di Piazza, E.; Merhi, A.; Norel, L.; Choua, S.; Turek, P.; Rigaut, S. *Inorg. Chem.* **2015,** *54* , 6347-6355.
(11) a) Motoyama, K.; Koike, T.; Akita, M. *Chem. Commun.* **2008**, 5812; b) Tanaka, Y.; Ishisaka, T.; Inagaki, A.; Koike, T.; Lapinte, C.; Akita, M. *Chem. Eur. J.* **2010**, *16*, 4762. c) Tanake, Y.; Inagaki, A.; Akita, M. *Chem. Commun.* **2007**, 1169-1171; d) Liu, Y.; Lagrost, C.; Costuas, K.; Tchouar, N.; Bozec, H. L.; Rigaut, S. *Chem. Commun.* **2008**, 6117-6119; d) Hervault, Y.; Ndiaye, C. M.; Norel, L.; Lagrost, C.; Rigaut, S. *Org. Lett.* **2012**, *14*, 4454-4457; e) Liu, Y.; Ndiaye, C. M.; Lagrost, C.; Costuas, K.; Choua, S.; Turek, P.; Norel, L.; Rigaut, S. *Inorg. Chem.* **2014**, *53*, 8172-8188; f) Mulas, A.; He, X.; Hervault Y. -M.; Norel, L.; Rigaut, S.; Lagrost, C. *Chem. Eur. J.* **2017** doi:10.1002/chem.201701903; g) Meng, F.; Hervault, Y.; Shao, Q.; Hu, B.; Norel, L.; Rigaut, S.; Chen, X. *Nat. Commun.* **2014**, *5*, 3023; h) Meng, F.; Hervault, Y.-M.; Norel, L.; Costuas, K.; Van Dyck, C.; Geskin, V.; Cornil, J.; Hng, H. H.; Rigaut, S.; Chen, X. *Chem. Sci.* **2012**, *3*, 3113-3138; i) Li, B.; Wang, J.Y.; Wen, H.-M.; Shi, L.-X.; Chen, Z.-N. *J. Am. Chem. Soc.* **2012**, *134*, 16059-16067.
(12) a) Browne W. R.; de Jong, J. J. D.; Kudernac, T. ; Walko, M.; Lucas, L. N.; Uchida, K.; van Esch, J. H.; Feringa, B. L., *Chem. Eur. J.* **2005**, *11*, 6414-6429; b) *Ibid*, 6430-6441; c) Guirado, G.; Coudret, C.; Hliwa, M.; Launay, J.-P. *J. Phys. Chem. B*, **2005**, *109*, 17445; d)Roberts, M. N.; Nagle, J. K.; Finden, J. G.; Branda, N. R.; Wolf, M. O. *Inorg. Chem.* **2008**, 48, 19-21.
(13) Note that attemps to stereoselectively close **1o** to **1c** in the solid state failed.
(14) See reviews on logic gates: a) Pilarczyk, K; Daly, B.; Podborska, A.; Kwolek, P.; A.D. Silverson, V.; de Silva, A. P.; Szacilowski, K. *Coord. Chem. Rev.* **2016**, *325*, 135-160; b) Andreasson, J.; Pischel, U. *Chem. Soc. Rev.* **2010** *39*, 174-188; c) Katz, E.; Privman, V. *Chem. Soc. Rev.* **2010**, *39*, 1835-1857; d) Szacilowski, K. *Chem. Rev.* **2008**, *108*, 3481-3548.
(15) For transition-metal based DTE systems, see: Harvey, E. C.; Feringa, B. L.; Vos, J. G.; Browne, W. R.; Pryce, M. T. *Coord. Chem. Rev.* **2015**, *282-283*, 77-86.